Electronic Supplementary Information

Highly Stable Interface Formation in Onsite Coagulation Dual-Salt Gel Electrolyte for Lithium-Metal Batteries

Yu-Hsing Lin,[a] Ramesh Subramani,[a] Yu-Ting Huang,[a] Yuh-Lang Lee,[a,b] Jeng-Shiung Jan,[a,b,*] Chi-Cheng Chiu,[a,b] Sheng-Shu Hou,[a,b,*] and Hsisheng Teng[a,b,c,*]

[a]Department of Chemical Engineering, National Cheng Kung University, Tainan 70101, Taiwan

[b]Hierarchical Green-Energy Materials (Hi-GEM) Research Center, National Cheng Kung University, Tainan 70101, Taiwan

[c]Center of Applied Nanomedicine, National Cheng Kung University, Tainan 70101, Taiwan.

*E-mail: hteng@mail.ncku.edu.tw

*E-mail: jsjan@mail.ncku.edu.tw

*E-mail: sshou@mail.ncku.edu.tw

Supporting information for:

1. SEM images of the separator and SGPE
2. Nyquist impedance plots of electrolytes
3. Raman spectra of electrolytes
4. t_{Li+} determination for dual-salt LE
5. Charge-discharge and impedance data of batteries during cycling
6. Full-range XPS spectra of SEI layers
7. Performance of SGPE pouch cell
8. Performance of Li|SGPE|NMC_{622}

1. SEM images of the separator and SGPE

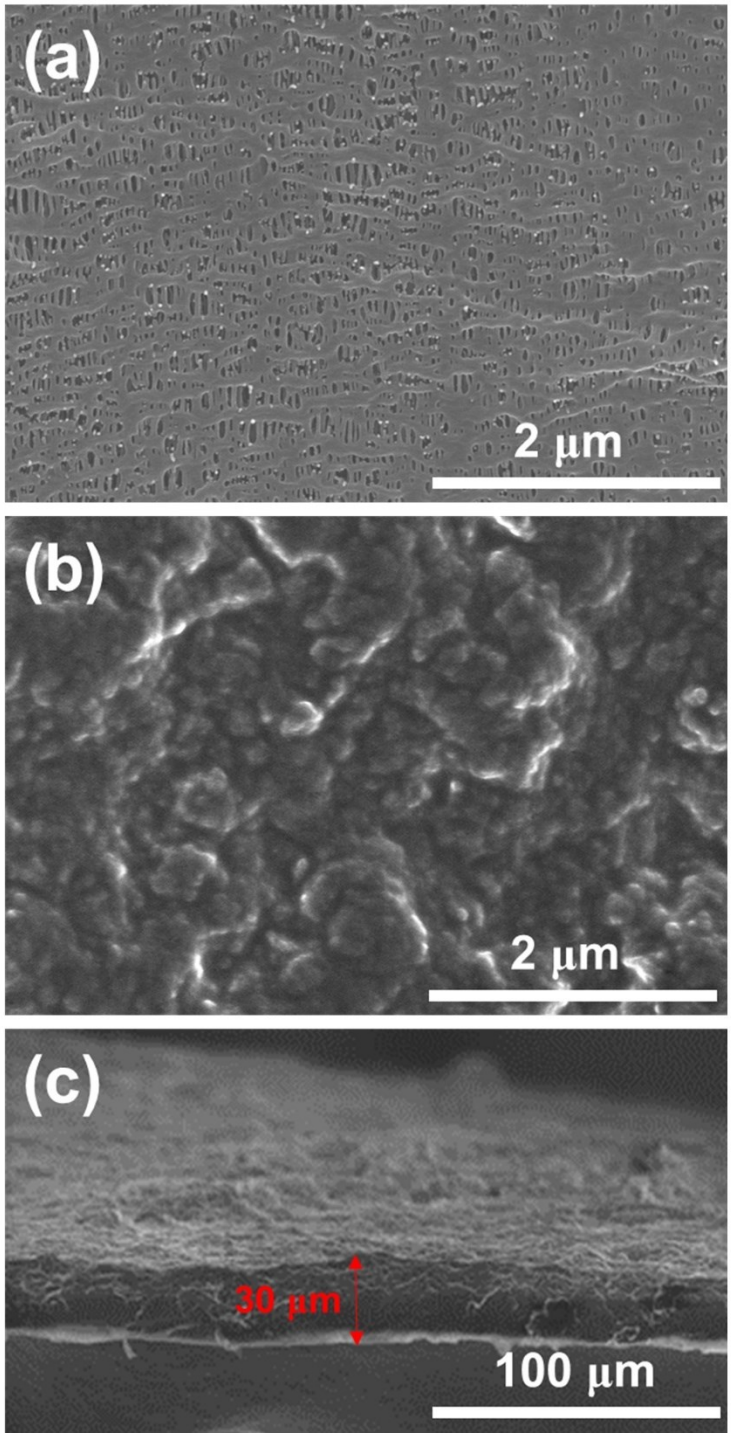

Fig. S1 SEM images of the separator and SGPE. (a) Top-view image of Celgard separator. (b) Top-view image of SGPE. (c) Cross-sectional image of SGPE.

2. Nyquist impedance plots of electrolytes

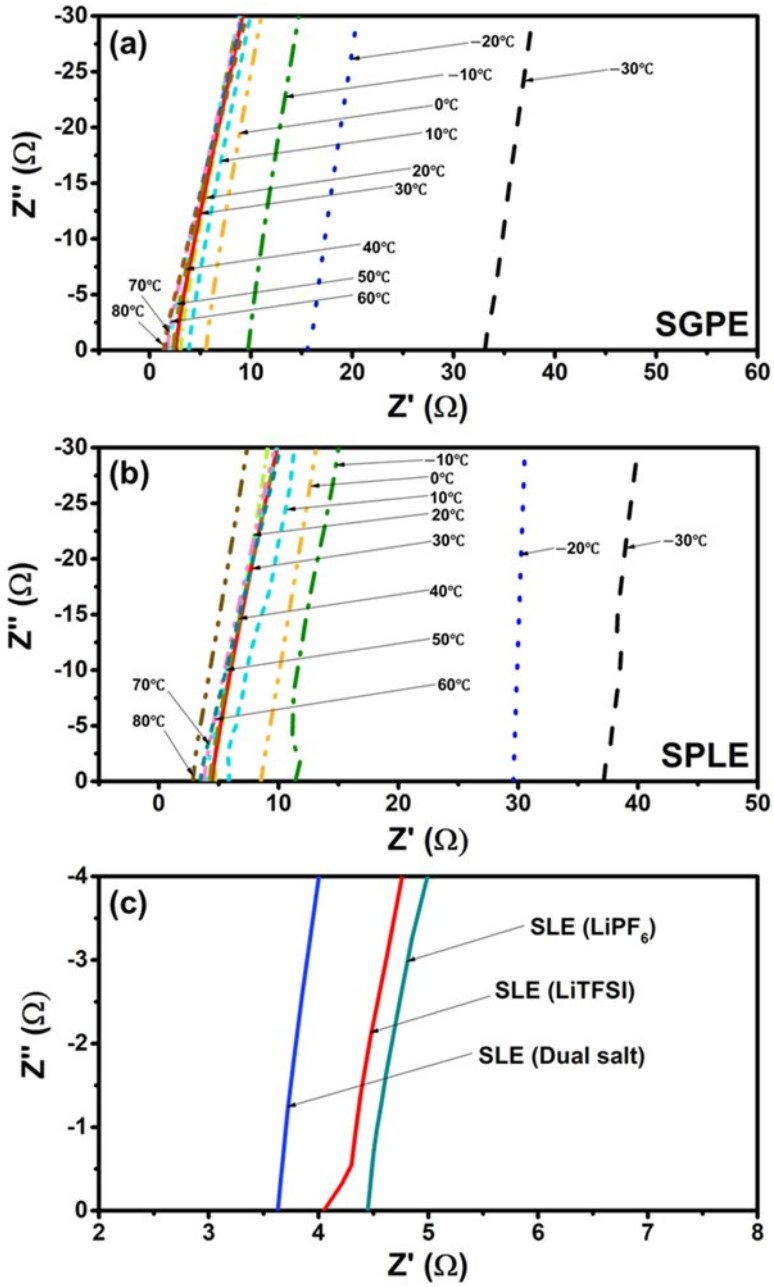

Fig. S2 Nyquist impedance plots of the electrolytes sanwiched between two SS foils. (a) SGPE at various temperatures. (b) SPLE at various temperatures. (c) The dual-salt, $LiPF_6$, and LiTFSI SLEs at room temperature. The analysis was conducted at 0 V with an AC potential amplitude of 10 mV over a frequency range of 100 mHz to 100 kHz.

3. Raman spectra of electrolytes

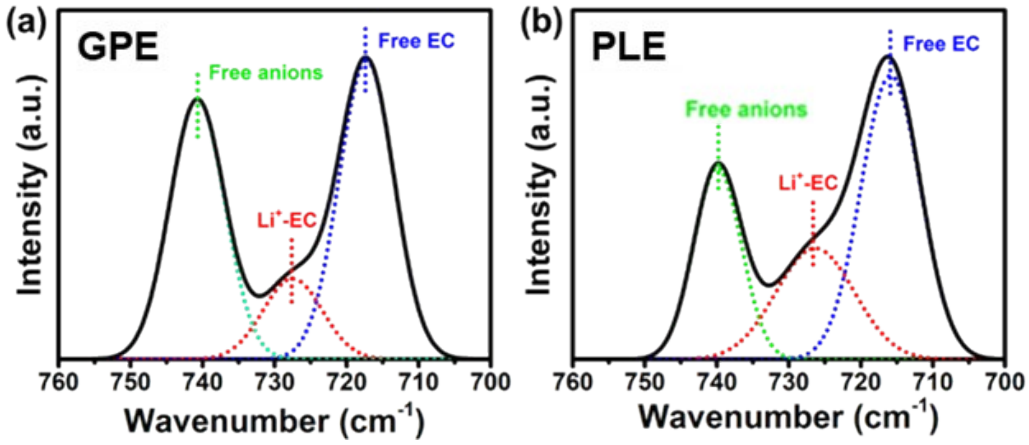

Fig. S3 Raman spectra (solid lines) of the electrolytes and the constituent peaks obtained through spectrum deconvolution (dotted lines) in the wavenumber regime of 700–760 cm^{-1}. (a) GPE. (b)PLE.

4. t_{Li+} determination for dual-salt LE

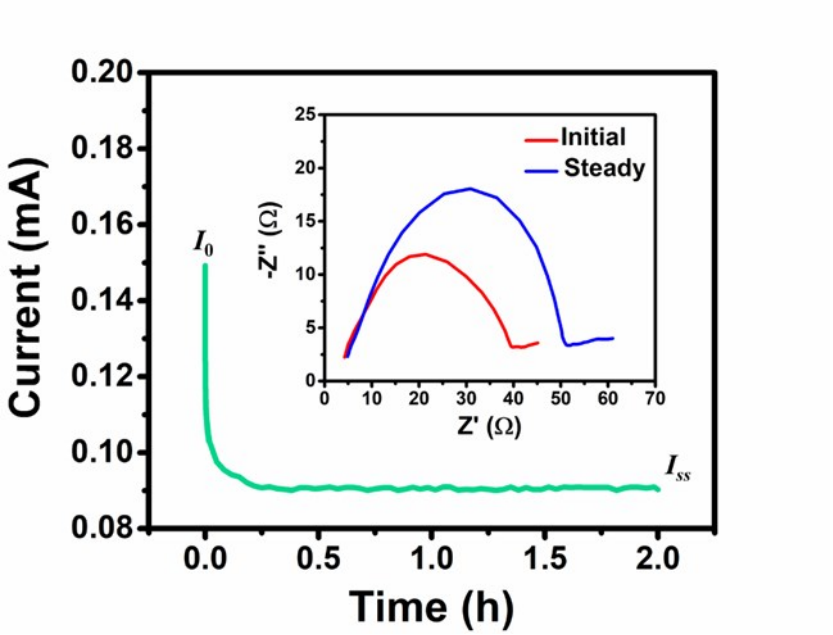

Fig. S4 Variations in the current and impedance of the Li|dual-salt LE|Li symmetric cells with time under polarization at 10 mV.

5. Charge-discharge and impedance data of batteries during cycling

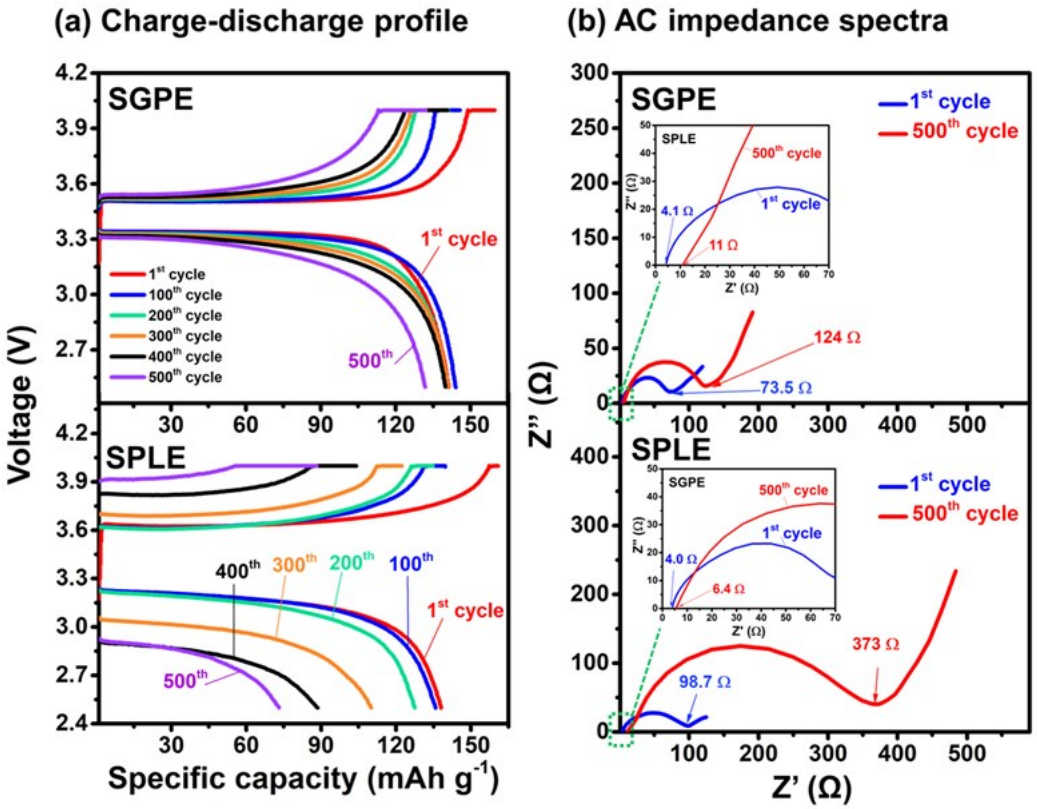

Fig. S5 Electrochemical performance of the Li||$LiFePO_4$ batteries during charge-discharge cycling. (a) Charge–discharge profiles of the Li|SGPE|$LiFePO_4$ and the Li|SPLE|$LiFePO_4$ batteries at different cycles. (b) AC impedance spectra of the Li|SGPE|$LiFePO_4$ and the Li|SPLE|$LiFePO_4$ batteries at different cycles. The batteries charged and discharged at 1 C for 500 cycles.

6. Full-range XPS spectra of SEI layers

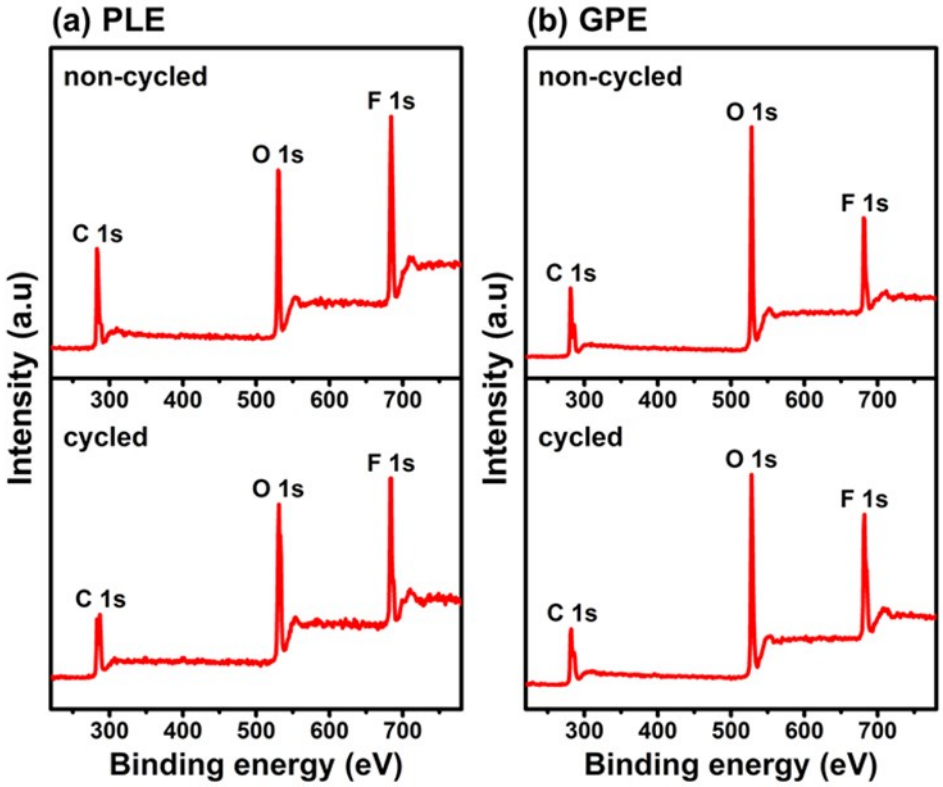

Fig. S6 Full-range XPS spectra of the SEI layer on the Li anodes in the Li||$LiFePO_4$ batteries. (a) Spectra of the SEI in the Li|SPLE|$LiFePO_4$ battery before and after cycling; (b) Spectra of the SEI in the Li|SGPE|$LiFePO_4$ battery before and after cycling. The noncycled batteries were aged for 48 h before being disassembled for analysis. The cycled batteries were aged for 48 h and subsequently charged and discharged at 1 C for 10 cycles before analysis.

7. Performance of SGPE pouch cell

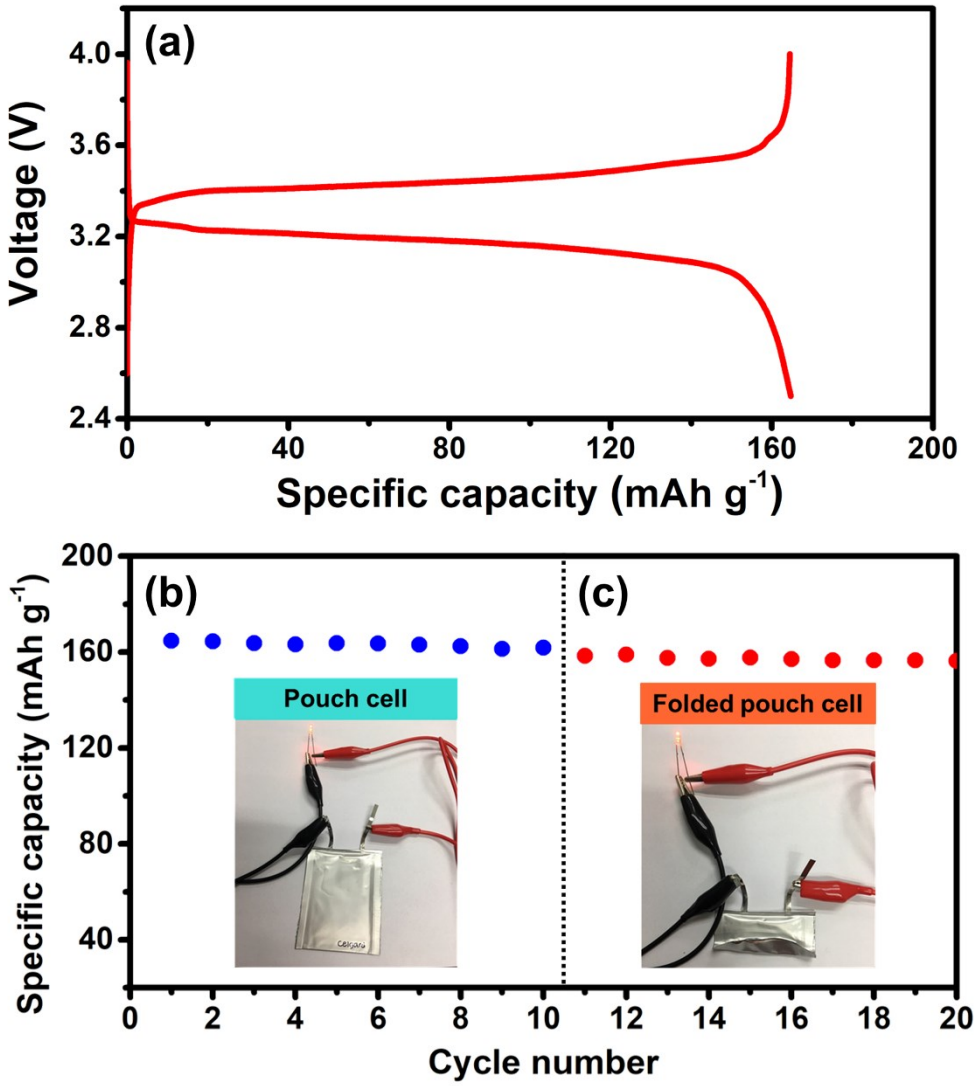

Fig. S7 The performance of the graphite|SGPE|$LiFePO_4$ pouch cell. (a) Charge–discharge profile of the cell, which was charged and discharged at 0.1C between 2.5 and 4.0 V. (b) Charge-discharge cycling performance of the cell at 0.1C and photograph of the cell to lighten an LED. (c) Charge-discharge cycling performance of the folded cell at 0.1C and photograph of the folded cell to lighten an LED.

8. Performance of Li|SGPE|NMC_{622}

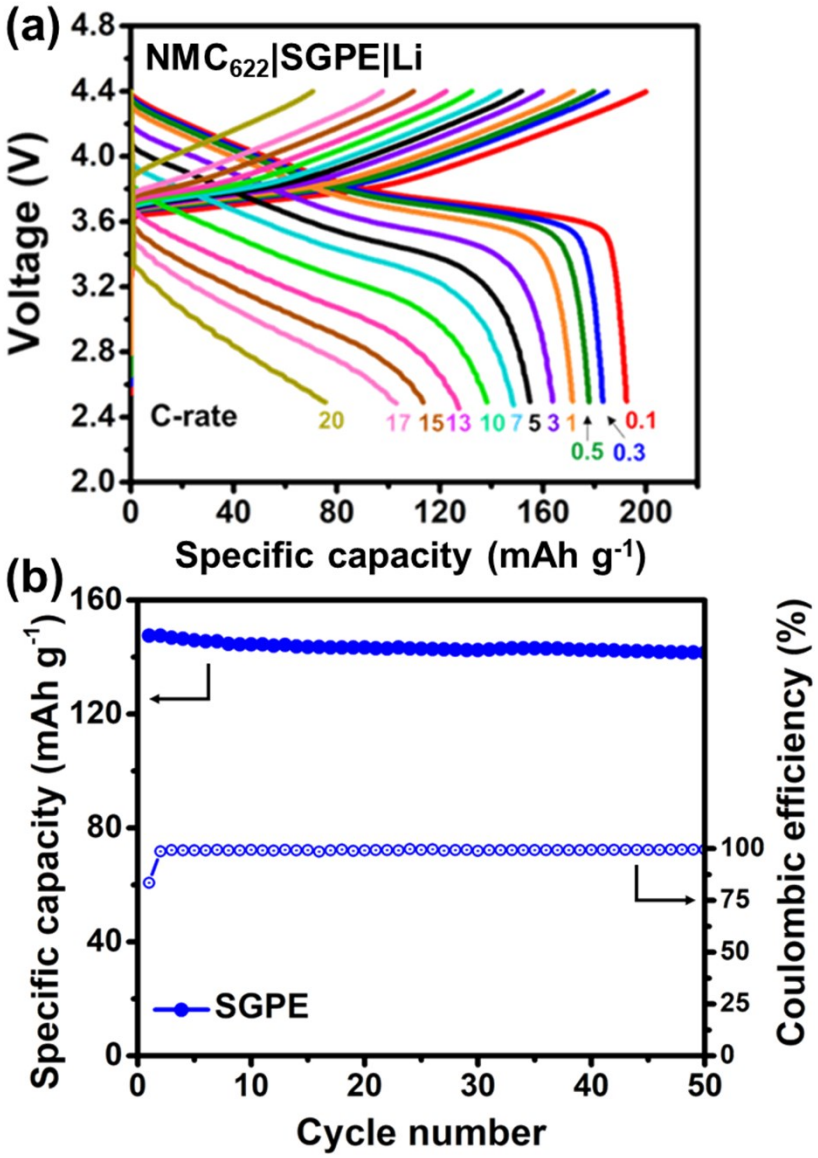

Fig. S8 The performance of Li|SGPE|NMC_{622} battery. (a) Charge–discharge profiles obtained with charging at 0.3C and discharged at various C-rates between 2.5 and 4.4 V. (b) Charge–discharge cycling performance at 1C for 50 cycles.